

Automating Deformable Gasket Assembly

Simeon Adebola^{*1}, Tara Sadjadpour^{*1}, Karim El-Refai^{*1}, Will Panitch¹, Zehan Ma¹,
Roy Lin¹, Tianshuang Qiu¹, Shreya Ganti¹, Charlotte Le¹, Jaimyn Drake¹, and Ken Goldberg¹

Abstract—In Gasket Assembly, a deformable gasket must be aligned and pressed into a narrow channel. Gasket Assembly is a long-horizon, high-precision task as the gasket must align with the channel and be fully inserted into the channel to achieve a secure fit. We present and compare 4 methods for Gasket Assembly: one policy from deep imitation learning and three procedural algorithms. We evaluate each method using 3D printed channels with 100 physical trials. Results suggest that deep imitation learning can fail (lowest quartile of alignment and insertion performance) on a straight channel in 2 of 10 trials, whereas a hybrid procedural algorithm achieves highest quartile performance in all 10 trials. The procedural algorithm also performs reliably on a curved channel but poorly on a closed trapezoidal channel. Code, videos, and data can be found at this url.

I. INTRODUCTION

Interactions with deformable objects encompass a broad range of tasks in robotic settings, such as clothes folding, thread untangling, and cable tracing. One such deformable manipulation task is the assembly of *gaskets*, small deformable components that fill the space between two or more mating surfaces to provide a seal, generally to prevent leakage from or into the joined objects while under compression [1]. Gaskets play critical roles in industries such as automotive and appliance manufacturing (where they are essential for sealing windows, engines, and fuel systems), plumbing, power generation, and construction.

To properly assemble a gasket, a robot must pick and place the gasket, a 1D deformable object, into a channel of similar length and width, such that the gasket snugly and completely fills the entire channel. The task requires multiple pick-and-place, press, and slide moves to be performed on the same deformable object in succession. The gasket assembly problem is a high-precision long-horizon task with a large state space, complicated dynamics, and low error tolerances. Almost all gasket assembly today is performed by humans.

We explore how this task can be automated. We propose a learned implementation and three procedural algorithms. We compare these on three testbeds of increasing difficulty.

This paper makes the following contributions:

- 1) A novel formulation of a gasket assembly task.
- 2) A deep imitation learning policy generated from 250 human-teleoperated demonstrations.
- 3) Three analytic/procedural algorithms for the same task
- 4) Experimental results comparing the learned policy and the procedural algorithms in 100 physical trials.

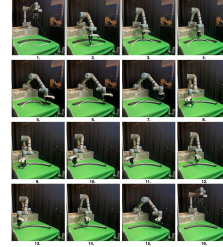


Fig. 1: **Gasket Assembly Example.** The robot picks, places and presses the gasket into the channel at various points until full assembly.

II. RELATED WORK

A. Routing Tasks with DLOs

In this paper, we focus on the 1D class of deformable objects, also known as deformable linear objects (DLOs), since they best represent gaskets. We use the terms “DLO” and “gasket” interchangeably in this paper. A common task category for 1D deformable manipulation is routing, in which a DLO is manipulated to match a given set of position and shape constraints. Recent research has explored a range of techniques and approaches for “cable routing,” a process in which a cable is guided along a path by a series of unconnected fixtures [2–6]. Gasket Assembly demands a greater level of accuracy in both perception and manipulation, highlighting the need for advanced techniques capable of handling the intricacies of secure gasket insertion.

B. Deep Imitation Learning and Diffusion Policy

Imitation learning from human demonstrations is one of the predominant approaches to learning robot visuomotor policies. Diffusion Policy [7], motivated by the powerful generative modeling capabilities of diffusion models [8, 9], was recently proposed to represent a robot’s visuomotor policy as a conditional denoising diffusion process. It learns the gradient of the action-distribution score function during training and iteratively performs a series of stochastic Langevin dynamics steps during inference. Specifically, starting from \mathbf{a}^K sampled from Gaussian noise, the Denoising Diffusion Probabilistic Model (DDPM) performs K iterations of denoising to produce intermediate vectors with decreasing levels of noise, $\mathbf{a}^K, \mathbf{a}^{K-1}, \dots, \mathbf{a}^0$, until a desired noise-free output \mathbf{a}^0 is obtained. Mathematically, to learn the conditional distribution $p(\mathbf{a}_t | \mathbf{o}_t)$, where \mathbf{o}_t is the observation of the current step and \mathbf{a}_t is the desired action output, we use a conditional CNN $\epsilon_\theta(\mathbf{a}^k, k | \mathbf{o})$ to get

$$\mathbf{a}^{k-1} = \alpha(\mathbf{a}^k - \gamma\epsilon_\theta(\mathbf{a}^k, k, \mathbf{o}) + \mathcal{N}(0, \sigma^2 I)),$$

^{*}Equal Contribution

¹The AUTOLab at UC Berkeley (automation.berkeley.edu)
{simeon.adebola, goldberg} @berkeley.edu

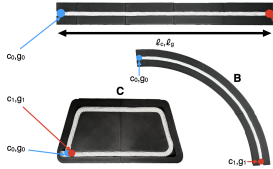


Fig. 2: **Channels and Gaskets in Goal Positions.** The straight channel (A) and the curved channel (B) are both open-ended channels whereas the trapezoid channel (C) is closed.

where α, γ, σ are noise schedule hyperparameters and functions of the iteration step k . During training, we minimize

$$\mathcal{L} = MSE(\epsilon^k, \epsilon_\theta(\mathbf{a}^k, k, \mathbf{o})),$$

where ϵ^k is a random noise with appropriate variance.

III. THE GASKET ASSEMBLY PROBLEM

An automated system must efficiently and reliably insert a gasket into a rigid channel of predefined shape and length. Both the channel and the gasket are continuous. In this paper, we consider gaskets with circular cross-sections. Unlike wires and most cables, gaskets are deformable in cross section, further differentiating Gasket Assembly from tasks like cable routing. We consider two performance metrics: (1) Alignment: How well does the gasket align with the target shape of the channel? and (2) Insertion: How much of the gasket is contained within the channel?

As shown in Figure 2, given an RGB image of the workspace, a gasket of fixed length l_g and maximum (circular) cross sectional diameter d , and a channel of width w , length l_c , and depth at least d , we attempt to insert the entire volume of the gasket into the channel such that the gasket is completely contained within the channel. We assume that $l_g \approx l_c$ and $w \leq d \leq w + \delta$, where δ is a deformation constant determined by the cross-sectional compressability of the gasket. These constraints ensure that d can be deformed to securely fit into w .

We denote the endpoints of the gasket as g_0 and g_1 , and select two points in the channel, which we denote as c_0 and c_1 . When the channel is open-ended (see Section V-B and Figure 2 A,B) g_0 and g_1 correspond to the two endpoints of the channel; however, when the channel is closed (Figure 2 C), g_0 and g_1 correspond instead to adjacent points in the channel such that the inserted gasket, taking the *longer* path between the two points, creates a closed loop.

We additionally constrain the problem space by assuming access to a priori knowledge of the shapes and dimensions of possible channels, a non-adversarial (no sharp corners, knots, or crossings) gasket starting configuration located within the reachable workspace of the robot and the field of view of the camera, and that the gasket and the channel can be easily color segmented from the workspace.

IV. ALGORITHMS

A. Learning Diffusion Policy

We collect and train on 250 demonstrations with the UR5 robot that is attached to a Robotiq gripper and mounted on

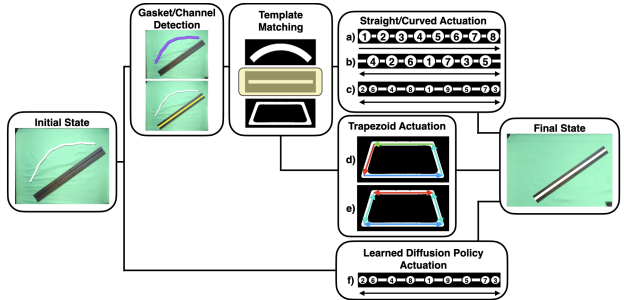


Fig. 3: The procedural algorithms consist of gasket/channel detection, template matching and then actuation. The Gasket/Channel Detection box shows gasket segmentation (above) and channel segmentation (below). The Straight/Curved Actuation box shows selection and actuation insertion strategies for the straight and curved channels: (a) is Unidirectional, (b) is Binary search, and (c) is Hybrid. The numbered circles on the channels represent the order and location where the robot attempts to place and press the gasket into. The arrows indicate the direction(s) of the slide(s). For the trapezoid channel, we treat each trapezoid segment as an instance of the straight channel (d,e). The learned policy proceeds directly from the initial state to actuation (f). The Final State box shows the final assembled gasket.

a metal base. We use three cameras: two ZED 2s and a Logitech BRIO webcam. One ZED 2 is mounted above the workspace and the other ZED 2 is mounted off to the left of the workspace, with the UR5 and workspace fully in view. The Logitech webcam is mounted on the wrist of the UR5. A human operator teleoperates the robot using a 3D mouse. We use the codebase from [10] for the system.

After collecting 250 demonstrations, we use a CNN-based model architecture for Diffusion Policy with an action prediction horizon of 16 and observation history length of 2. $\epsilon_\theta(\cdot)$ takes in the noisy action $\mathbf{a}_{t,t+1,\dots,t+15}^k$ and uses a few 1D convolutional layers with FiLM conditioning [11] on the observation embeddings. Details are in the original paper [7]. After training, we get a policy that successfully carries out the Gasket Assembly task.

B. 3 Procedural Algorithms

1) *Perception:* The perception system aims to detect, separate, and localize the channel and gasket given an RGB image from an overhead workspace camera. Since we know the channel shape, we use a template matching algorithm for channel localization and identification. To enable this, we generate a ground truth binary mask and aspect ratio for each channel by using the CAD source files for each part. These ground truth masks are passed to the perception pipeline and used in the classification and planning steps. Our approach is broken into: Segmentation and Classification, Localization via Alignment, Skeletonization, and Waypoint Selection.

2) *Robot Primitives:* We define a small set of versatile primitives to enable efficient environment interaction: Pick and Place, Shift and Place, Press, Slide, and Home.

3) *3 Insertion Algorithms:* **Unidirectional** insertion(Fig. 3a), **binary search** insertion(Fig. 3b), and a **hybrid** of the two methods(Fig. 3c).

- (i) Unidirectional insertion: The robot picks, places, and inserts the gasket into the channel, starting at one end of the gasket and progressing toward the other end. Then, the robot presses each selected point of the gasket into

the channel for a second time to reinforce the insertion. Finally, the robot slides its gripper along the entire length of the channel to seal the gasket.

- (ii) Binary search insertion (Fig. 3b): The robot begins by picking and placing the midpoint of the gasket, followed by the points located at $\frac{1}{4}$ and $\frac{3}{4}$ of the gasket length, followed by those at the eighths, and so on until the algorithm reaches a termination limit (we set $\frac{1}{8}$ for the straight and curved channels, and $\frac{1}{4}$ for the trapezoid channel). Then, the robot presses each selected point of the gasket into the channel in the same order as they were picked and placed to reinforce the insertion. Lastly, the robot performs a “binary slide” by starting at the midpoint and sliding once toward each end.
- (iii) Hybrid insertion (Fig. 3c): This method attempts to combine the advantages of the unidirectional and binary search approaches. The robot begins by picking, placing, and inserting the midpoint of the gasket, followed by the endpoints. The robot then places the quarter and eighth points, as in the binary method. Then, the second reinforcing presses follow the unidirectional method. Finally, the binary slide is performed.

V. PHYSICAL EXPERIMENTS

A. Experimental Setup

We utilize a Universal Robots UR5 to conduct experiments. For Trials 1-10, the channel is at a fixed pose of 0° . For Trials 11-100, the position and orientation of the channel are randomized at the beginning of each trial to any location completely within the reachable workspace and any angle within $\theta = \pm 45^\circ$ of the horizontal, respectively.

At the beginning of all 100 trials, the starting position of the gasket is randomized. We perform this randomization by lifting the gasket with one fist and dropping it over either the top or bottom half of the workspace. The ends of the gasket are then moved outwards until the configuration of the gasket conforms to all of the constraints specified in Section III.

B. Channels and Gasket

We consider 3 channels in increasing order of difficulty, as shown in Fig. 2. Fig. 2A: The first channel is an open straight channel with dimensions 26.5" x 2.68" x 0.56". Fig. 2B: The second channel is an open curved strut channel covering a 90° arc of a circle, with inner diameter 32.4", outer diameter 35.1", and height 0.75". This results in a channel with dimensions analogous to that of the straight channel. Fig. 2C: Our third channel is a closed trapezoidal channel with a Long side of 10", a short side of 7.5", and two 4.5"-long non-parallel sides. All channels have an inner channel width of 0.5". We use a white 0.5" braided nylon rope as our gasket analogue. The rope is cut to a length of 26.5" to precisely match the length of the testbed channels.

C. Experimental Metrics

After the robot execution has terminated, a human judge rates performance into one of four categories for alignment and insertion and follows:

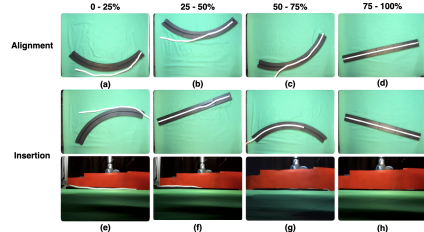


Fig. 4: **Metric Examples.** We provide examples for all four buckets of the alignment and insertion evaluation metrics. We show the final gasket and channel states after the robot attempts gasket assembly.

- 1) **0% - 25%:** A **major failure**, in which the robot has successfully aligned or inserted **less than 25%** of the gasket with the channel.
- 2) **25% - 50%:** A **partial failure**, in which **between 25% and 50%** of the gasket is successfully aligned or inserted.
- 3) **50% - 75%:** A **partial success**, in which **between 50% and 75%** of the gasket is properly aligned or inserted.
- 4) **75% - 100%:** A **full success**, in which the robot has properly aligned or inserted **at least 75%** of the gasket length with the channel.

D. Results

Following the evaluation metric in V-C, we perform 100 physical trials: 10 for the learned diffusion policy on the straight channel in fixed 0° pose and 90 across all procedural approaches and all channel types with varying channel pose positions and orientations as noted in Section V-A. Please see results in Tables I and II. Additionally, Figure 4 shows qualitative results from the trials of the three analytical algorithms in decreasing order of success. We note that the learned policy was only evaluated for the straight channel in a fixed channel pose since this matched the pose used during data collection whereas for the procedural algorithms, the channel pose varied significantly.

For the straight channel, the binary and hybrid approaches achieve 75-100% in all trials. For the curved channel, the hybrid approach separates itself from the binary search approach, attaining the highest alignment and insertion performance. Finally, for the most difficult channel, the trapezoid, the hybrid approach attains the best alignment performance, while having the same outcomes as the binary search for the insertion performance.

Trial	Channel	Method	Alignment Performance			
			0-25%	25-50%	50-75%	75-100%
1-10	Straight	Diff. Policy	2	0	0	8
11-20	Straight	Unidirectional	6	0	1	3
21-30	Straight	Binary Search	0	0	0	10
31-40	Straight	Hybrid	0	0	0	10
41-50	Curved	Unidirectional	5	1	0	4
51-60	Curved	Binary Search	0	0	4	6
61-70	Curved	Hybrid	0	0	1	9
71-80	Trapezoid	Unidirectional	10	0	0	0
81-90	Trapezoid	Binary Search	9	1	0	0
91-100	Trapezoid	Hybrid	9	0	1	0

TABLE I: Alignment Performance of 100 Physical Trials.

Trial	Channel	Method	Insertion Performance			
			0-25%	25-50%	50-75%	75-100%
10	Straight	Diff. Policy	2	0	1	7
20	Straight	Unidirectional	6	0	0	10
30	Straight	Binary Search	0	0	0	10
40	Straight	Hybrid	0	0	0	10
50	Curved	Unidirectional	7	0	1	2
60	Curved	Binary Search	1	3	6	0
70	Curved	Hybrid	0	0	1	9
80	Trapezoid	Unidirectional	10	0	0	0
90	Trapezoid	Binary Search	9	1	0	0
100	Trapezoid	Hybrid	9	1	0	0

TABLE II: Insertion Performance of 100 Physical Trials.

VI. LIMITATIONS + FUTURE WORK

In this paper, we present a new problem called Gasket Assembly. We provide results from 4 methods, namely a learned diffusion policy and 3 procedural techniques. In the future, we will perform more experiments varying channel pose for the diffusion policy and learning diffusion policies for the curved and trapezoidal channels. We also plan to better handle recovery from poorly executed primitives by exploring additional approaches including hierarchical imitation learning [6] and self-supervised learning. We will also explore more complex channel shapes including in cases where the shapes may not be known beforehand which will allow us to explore other algorithms apart from a template matching algorithm, and additional evaluation approaches.

REFERENCES

- [1] N. Aibada, R. Manickam, K. K. Gupta, and P. Raichurkar, “Review on various gaskets based on the materials, their characteristics and applications,” *Int. J. Text. Eng. Process*, vol. 3, no. 1, pp. 12–18, 2017.
- [2] S. Jin, W. Lian, C. Wang, M. Tomizuka, and S. Schaal, “Robotic cable routing with spatial representation,” *IEEE Robotics and Automation Letters*, vol. 7, no. 2, pp. 5687–5694, 2022.
- [3] G. A. Waltersson, R. Laezza, and Y. Karayannidis, “Planning and control for cable-routing with dual-arm robot,” in *2022 International Conference on Robotics and Automation (ICRA)*, May 2022, pp. 1046–1052.
- [4] A. Monguzzi, M. Pelosi, A. M. Zanchettin, and P. Rocco, “Tactile based robotic skills for cable routing operations,” in *2023 IEEE International Conference on Robotics and Automation (ICRA)*, 2023, pp. 3793–3799.
- [5] A. Wilson, H. Jiang, W. Lian, and W. Yuan, “Cable routing and assembly using tactile-driven motion primitives,” in *2023 IEEE International Conference on Robotics and Automation (ICRA)*, 2023, pp. 10408–10414.
- [6] J. Luo, C. Xu, X. Geng, G. Feng, K. Fang, L. Tan, S. Schaal, and S. Levine, “Multi-stage cable routing through hierarchical imitation learning,” *IEEE Transactions on Robotics*, 2024.
- [7] C. Chi, S. Feng, Y. Du, Z. Xu, E. Cousineau, B. Burchfiel, and S. Song, “Diffusion policy: Visuomotor policy learning via action diffusion,” in *Proceedings of Robotics: Science and Systems (RSS)*, 2023.
- [8] J. Sohl-Dickstein, E. A. Weiss, N. Maheswaranathan, and S. Ganguli, “Deep unsupervised learning using nonequilibrium thermodynamics,” in *Proceedings of the 32nd International Conference on International Conference on Machine Learning - Volume 37*, ser. ICML’15, Lille, France: JMLR.org, 2015, pp. 2256–2265.
- [9] J. Ho, A. Jain, and P. Abbeel, “Denoising diffusion probabilistic models,” in *Proceedings of the 34th International Conference on Neural Information Processing Systems*, ser. NIPS’20, Vancouver, BC, Canada: Curran Associates Inc., 2020.
- [10] P. Wu, Y. Shentu, Z. Yi, X. Lin, and P. Abbeel, *Gello: A general, low-cost, and intuitive teleoperation framework for robot manipulators*, 2023.
- [11] E. Perez, F. Strub, H. De Vries, V. Dumoulin, and A. Courville, “Film: Visual reasoning with a general conditioning layer,” in *Proceedings of the AAAI conference on artificial intelligence*, vol. 32, 2018.